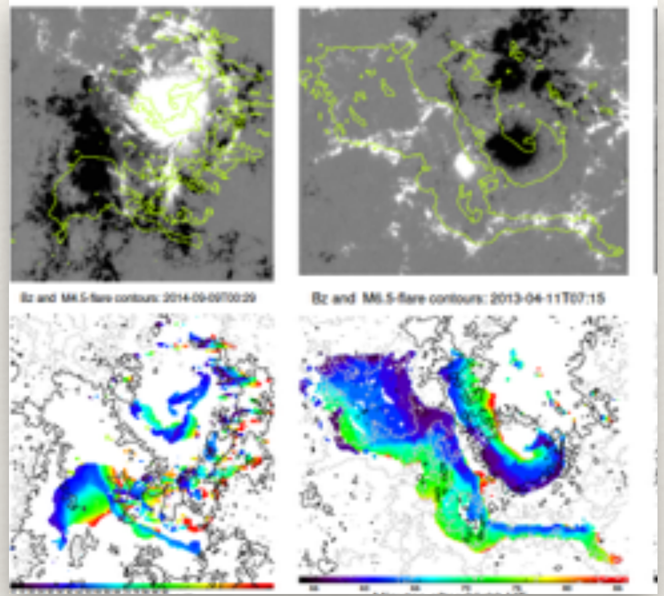

Online Seminar 22 Feb 2017, Ioffe Institute

A Database of Flare Ribbons Observed by Solar Dynamics Observatory

База данных свойств вспышечных лент, основанная на наблюдениях Солнечной Динамической обсерватории

Maria Kazachenko, Benjamin Lynch
Brian Welsch

UC Berkeley

Talk Outline

- Motivation: importance of flare ribbons; why now?
- Methods: deriving reconnection fluxes
- Database (~3000 events)
- Results
- Conclusions

Motivation: Standard Flare Model

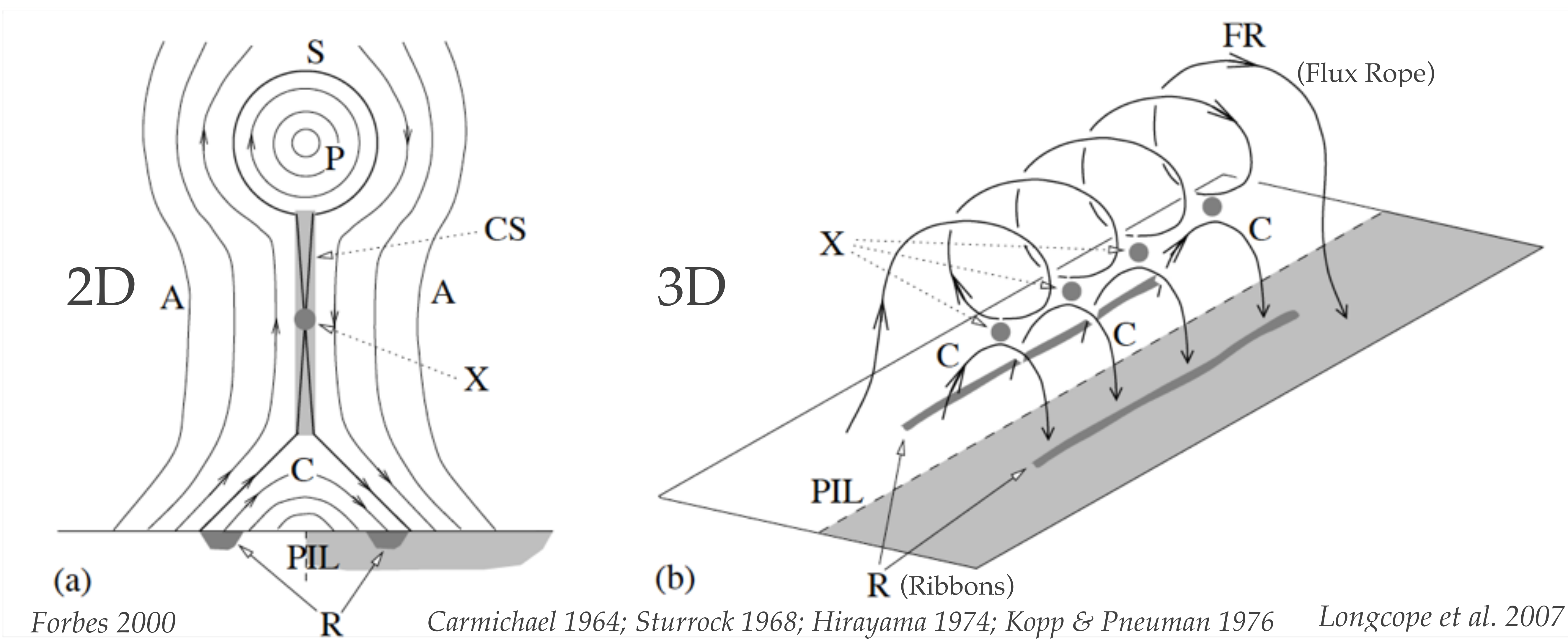

Flare Ribbons (R)— **footpoints of newly reconnected magnetic field lines** observed in chromospheric spectral lines (e.g AIA 1600A)

Reconnection flux rate:

$$\frac{d\Phi_r}{dt} = \frac{\partial}{\partial t}\int B_c dS_c = \frac{\partial}{\partial t}\int B_n dS_{\mathrm{ribbon}}$$

observed

corona photosphere

Forbes & Priest 1984

Past Observational Studies of Reconnected Flux Φ_R

Quantitative observational studies of reconnection flux Φ_R (e.g., Poletto & Kopp 1986; Fletcher et al. 2001; Isobe et al. 2005; Qiu & Yurchyshyn 2005; Fletcher et al. 2004; Saba et al. 2006; Qiu et al. 2007; Qiu 2009; Miklenic et al. 2009; Kazachenko et al. 2012, Hu et al. 2014).

<u>For example:</u>

V_{CME} : 13 events: strong correlation between Φ_R and the V_{CME}

Qiu & Yurchyshyn 2005

A_{CME}: 2 events: association between $d\Phi_R/dt$ and a_{CME}

Qiu et al. 2004

$\Phi_{MC,P}$: 9 events: $\Phi_R \sim \Phi_{MC,P}$ (poloidal flux of magnetic clouds)

Qiu et al. 2007

4 events: $\Phi_R \sim \Phi_{MC,P}$

Kazachenko et al. 2012

<u>Main Drawback: limited sample of events</u>

Motivation: SDO observations

Solar Dynamics Observatory: first time both a vector magnetograph (HMI) and ribbon-imaging capabilities (AIA) are available together.

- No time-consuming co-alignment
- Full-disk, 24 hours coverage.

Perfect time to assemble a much larger database of ribbon events (ribbon areas and reconnected fluxes) to more robustly examine the role of reconnection in flares and CMEs.

Some problems to overcome: saturation effects in AIA CCDs

Solution: We present a method to remove blooming from reconnection flux estimates.

Methodology: Correcting AIA Pixel Saturation.
Example of X2.2 flare in AR 11158

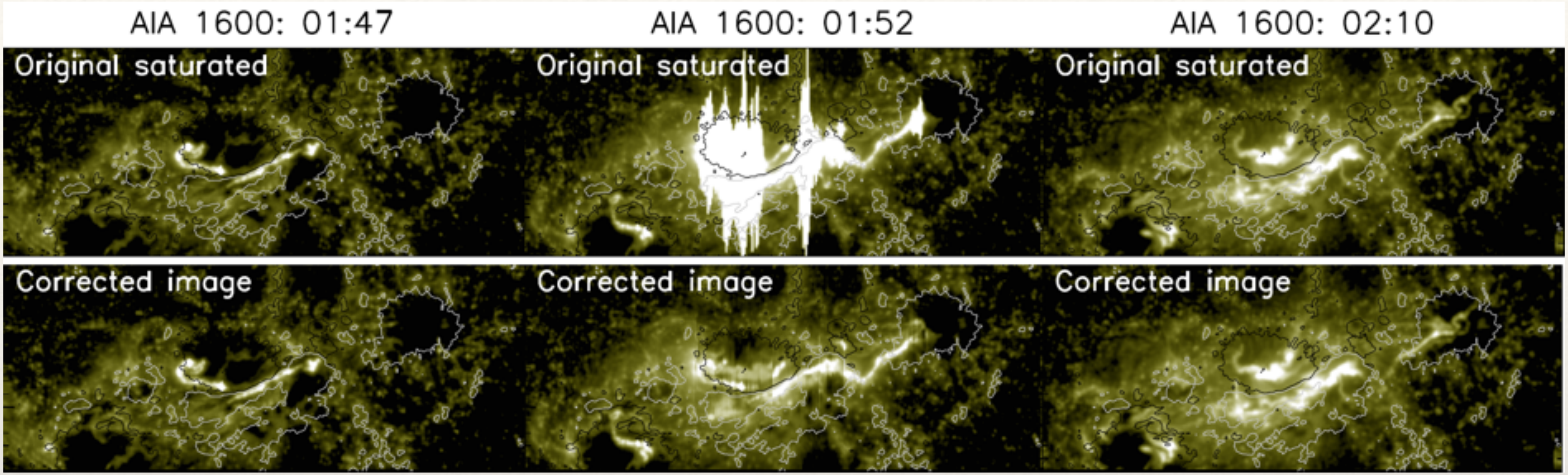

Background: Snapshots of the X2.2-flare ribbons in AR11158 observed at 1600A by AIA on 2011 February 15. Contours: HMI LOS fields.

1. AIA_PREP: Using the aia_prep.pro (IDL/SSW), process the UV 1600A images.
2. Original saturated: Co-align the AIA sequence in time by Fourier cross-correlation (e.g., Welsch et al. 2004)
3. Saturated pixels set to zero: Find saturated pixels, i.e. pixels above the threshold level (typically around 5000 counts/s) and set them to zero.
4. Corrected image: Linearly interpolate in time the values in each of the individually saturated pixels, using the signal when the pixel is not saturated.
5. Corrected image, ribbons only: select ribbon pixels (Qiu et. al 2002, Kazachenko et al. 2012)

Methodology: Calculating reconnection flux and flux rate
Example of X2.2 flare in AR 11158

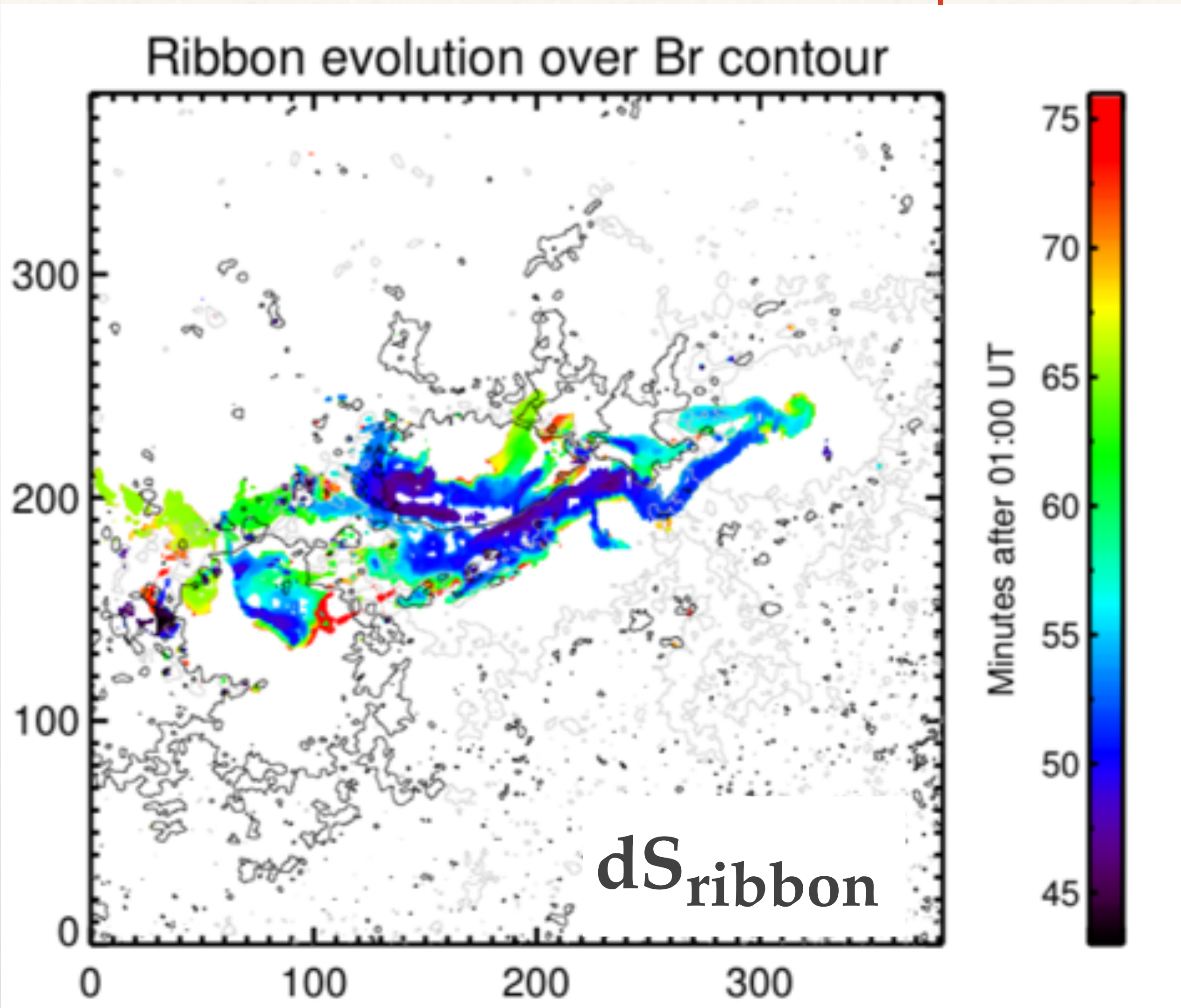

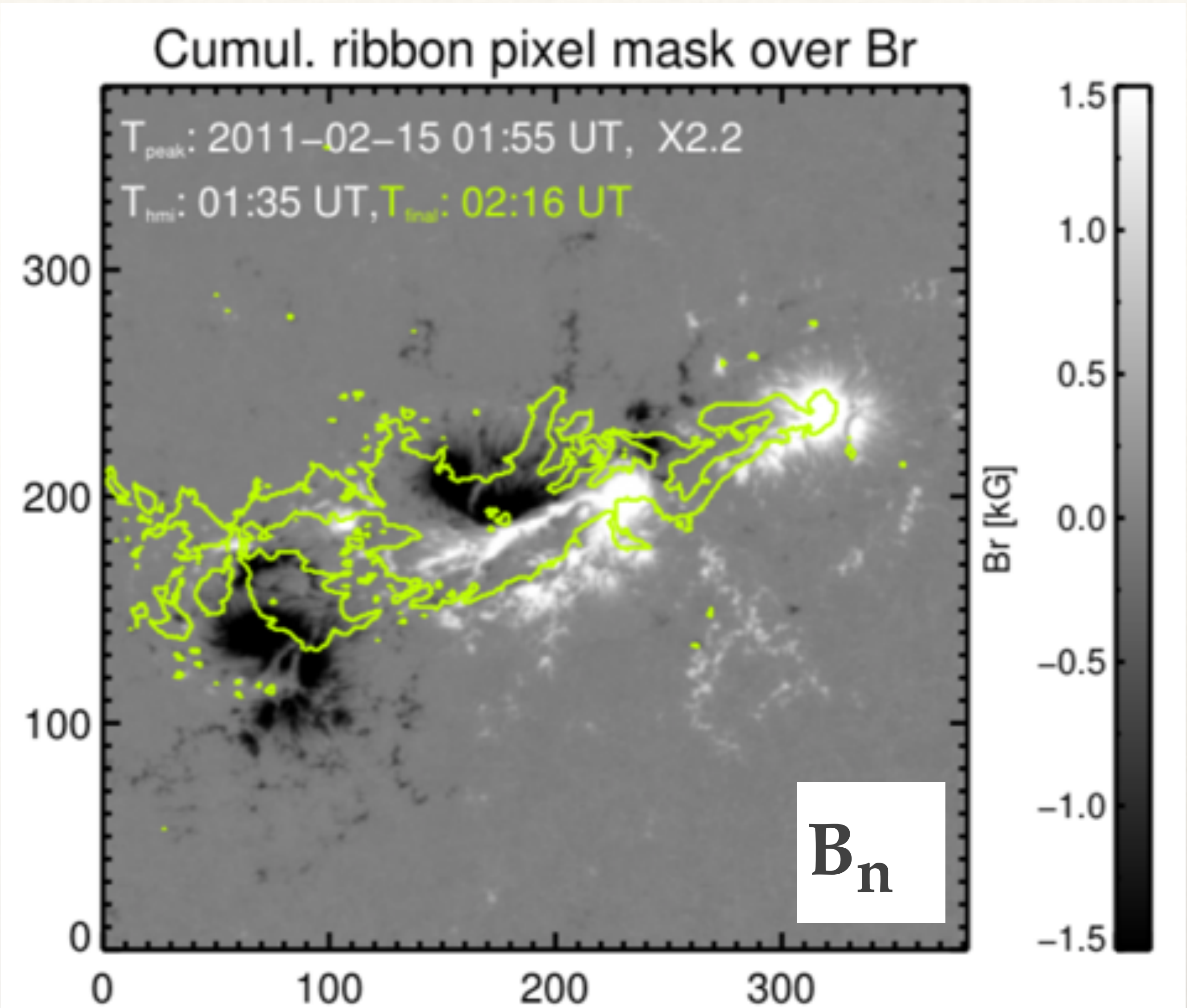

<u>Reconnected flux</u> (right panel)

$$\Phi_r(t) = \int B_n(t) dS_{ribbon}$$

Φ_R=5.7(-5.9)*10^{21} Mx.

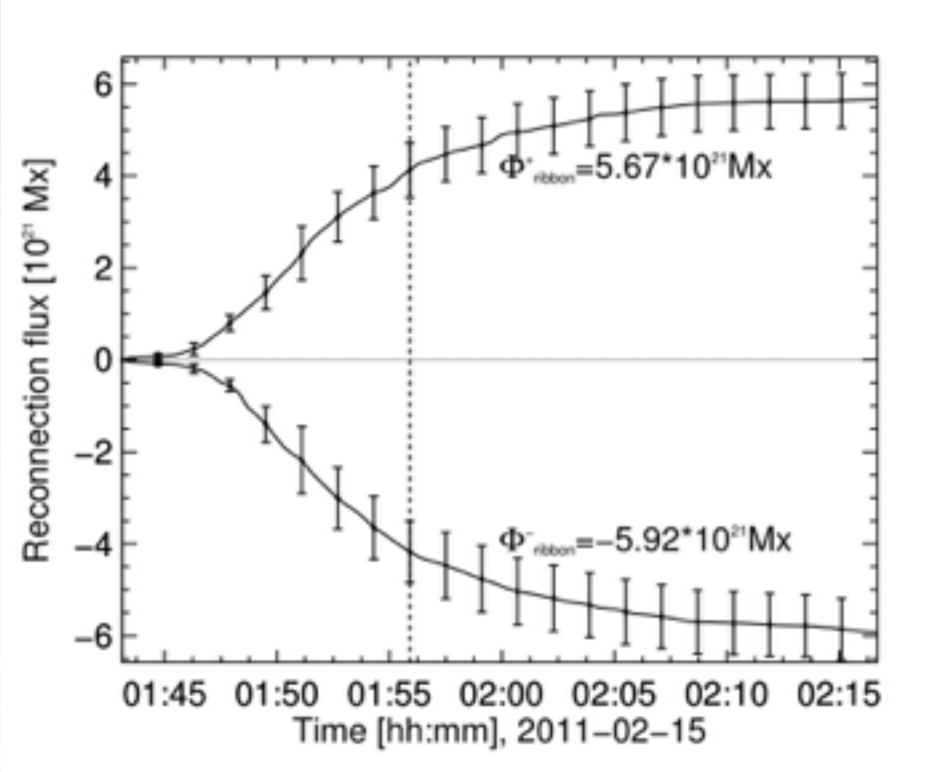

Database: selected flares

We selected all events >C1.0 within 45 degrees from the disk center:

3137 events: 17 X, 250 M and 2870 C-class flares

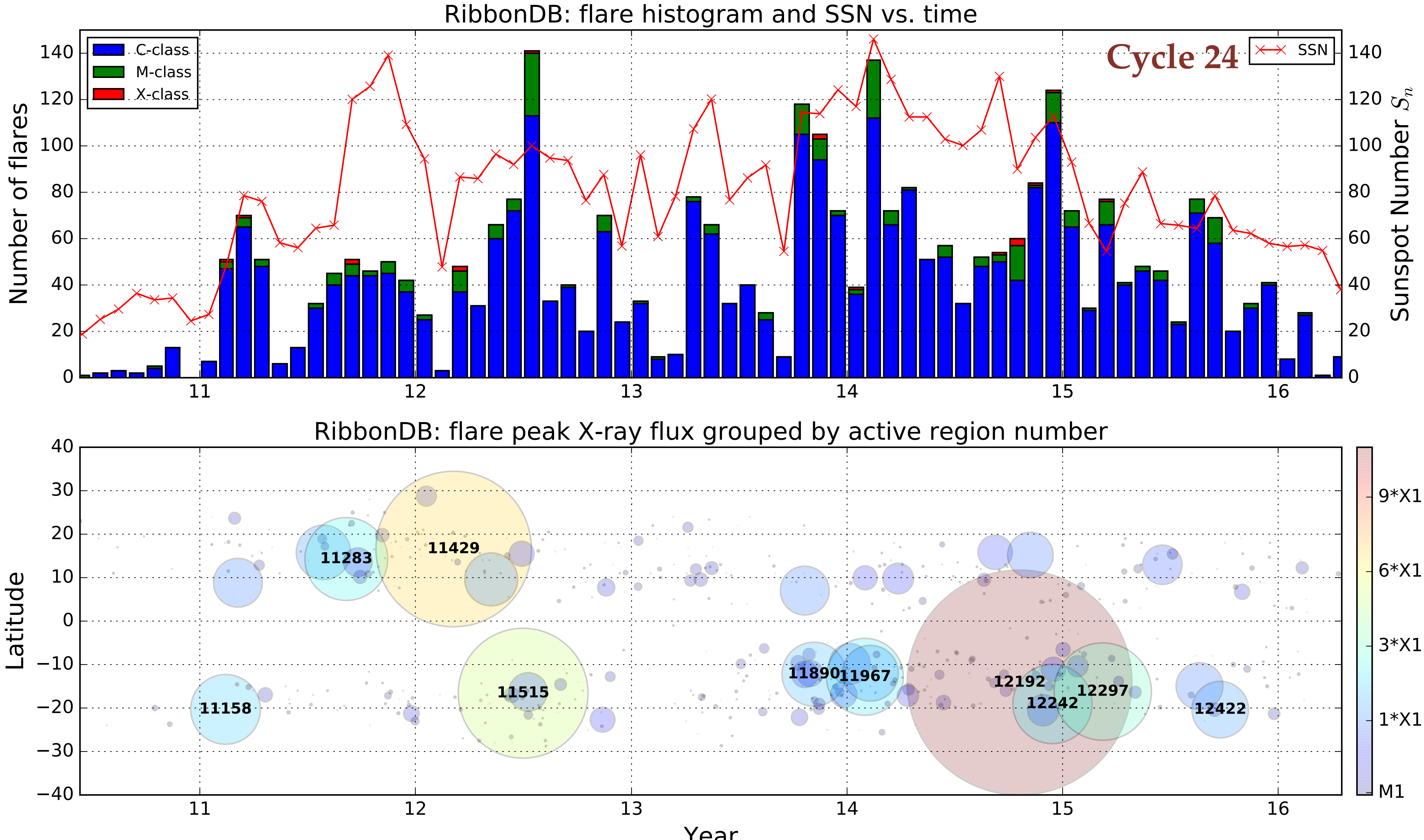

Kazachenko, Lynch, Welsch 2017

Database: derived quantities

- active region flux
- reconnection flux
- active region area
- ribbon area
- fraction of flux reconnected
- fraction of area reconnected

$$\Phi_{AR} = \int |B_n| dS,$$

$$\Phi_{\mathrm{ribbon}} = \int |B_n| dS_{\mathrm{ribbon}},$$

$$S_{\mathrm{AR}} = \int dS,$$

$$S_{\mathrm{ribbon}} = \int dS_{\mathrm{ribbon}},$$

$$R_{\Phi} = \frac{\Phi_{\mathrm{ribbon}}}{\Phi_{AR}} \times 100\%,$$

$$R_S = \frac{A_{rec}}{A_{AR}} \times 100\%,$$

Database examples: C1.6 and C3.9 flares

Radial magnetic field | Ribbon contour evolution | Reconnection flux

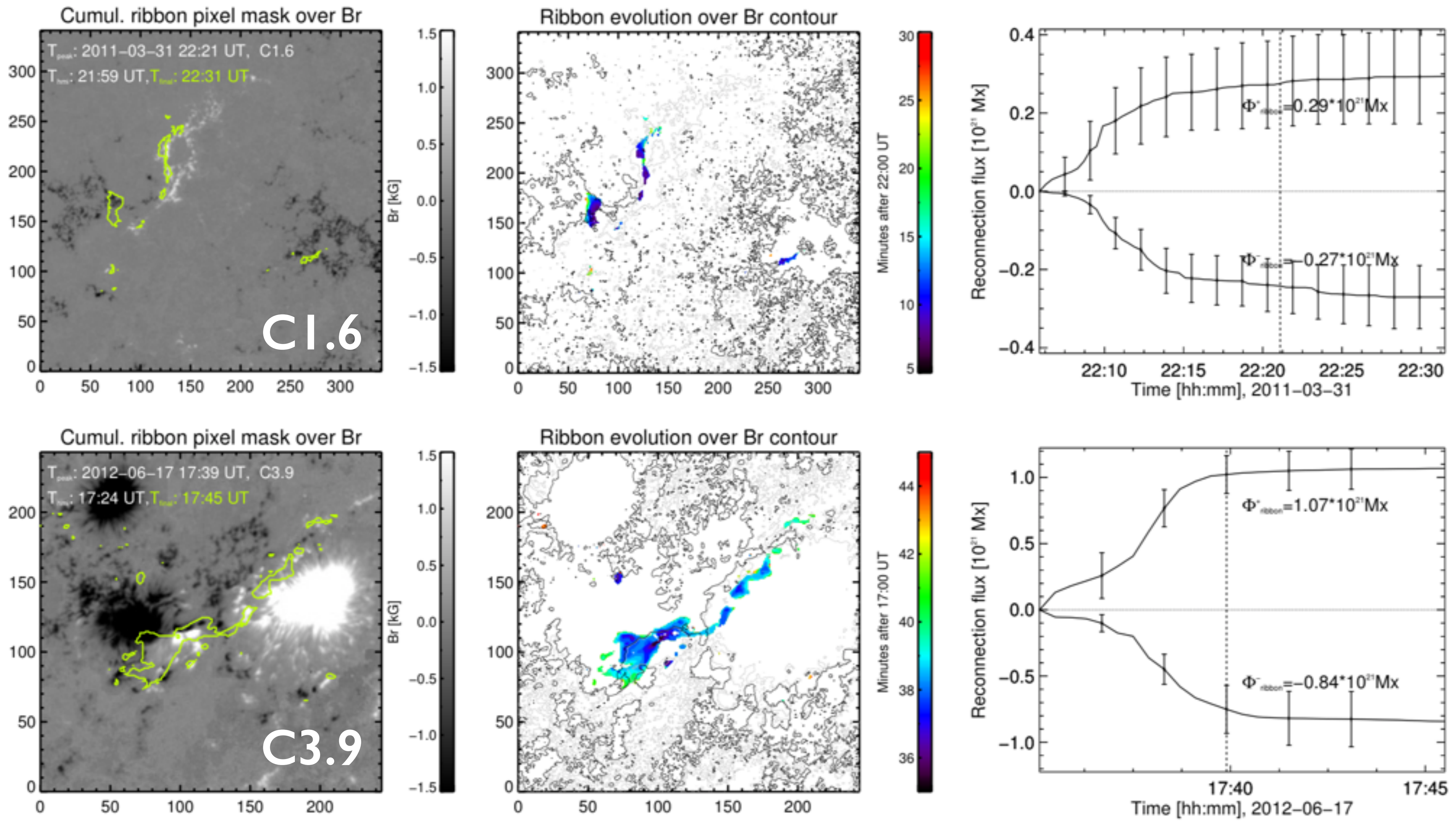

Database examples: M6.5 and X5.4 flares

Radial magnetic field | Ribbon contour evolution | Reconnection flux

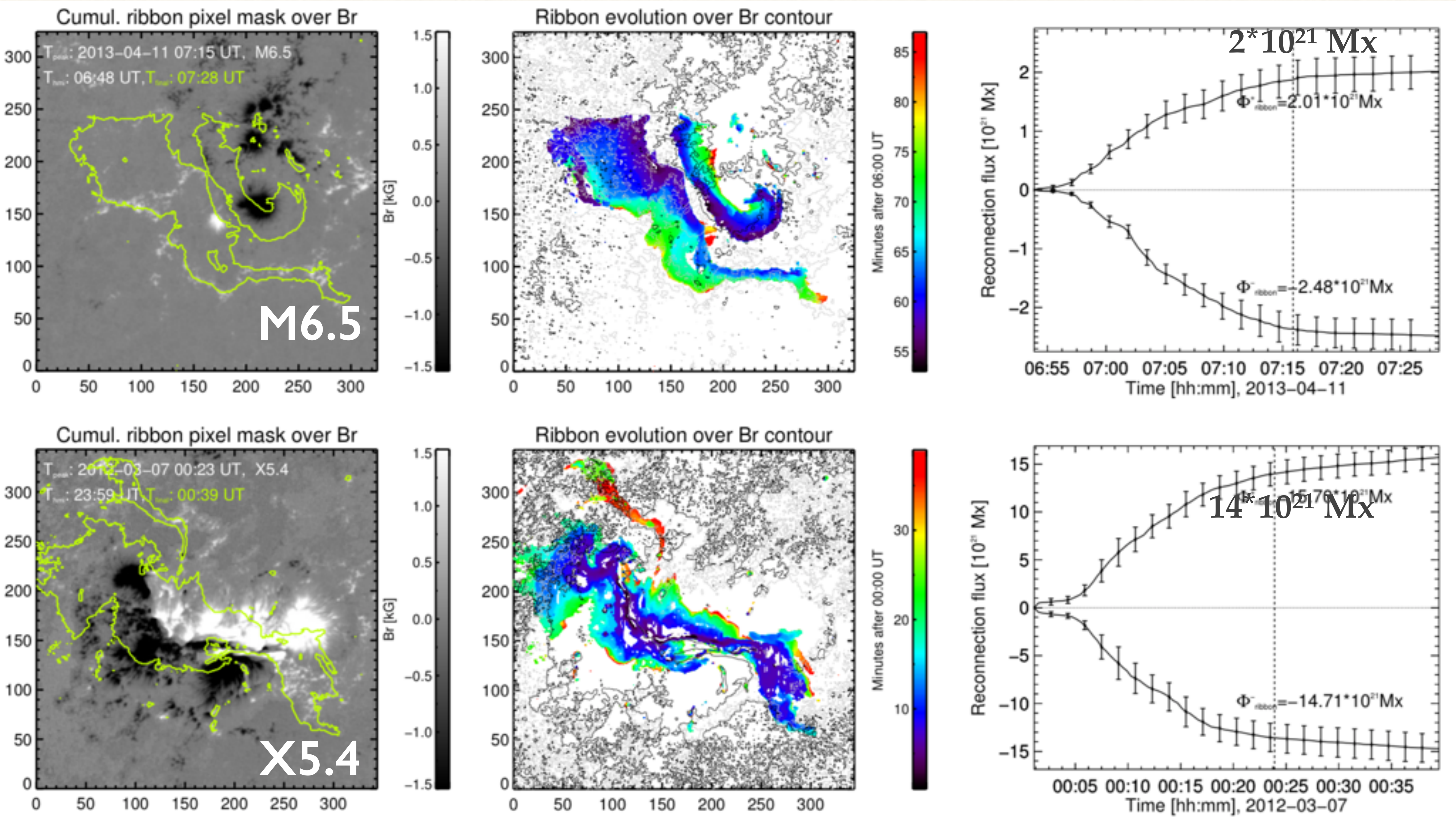

Results: Peak X-ray flux vs active region and reconnection magnetic fluxes

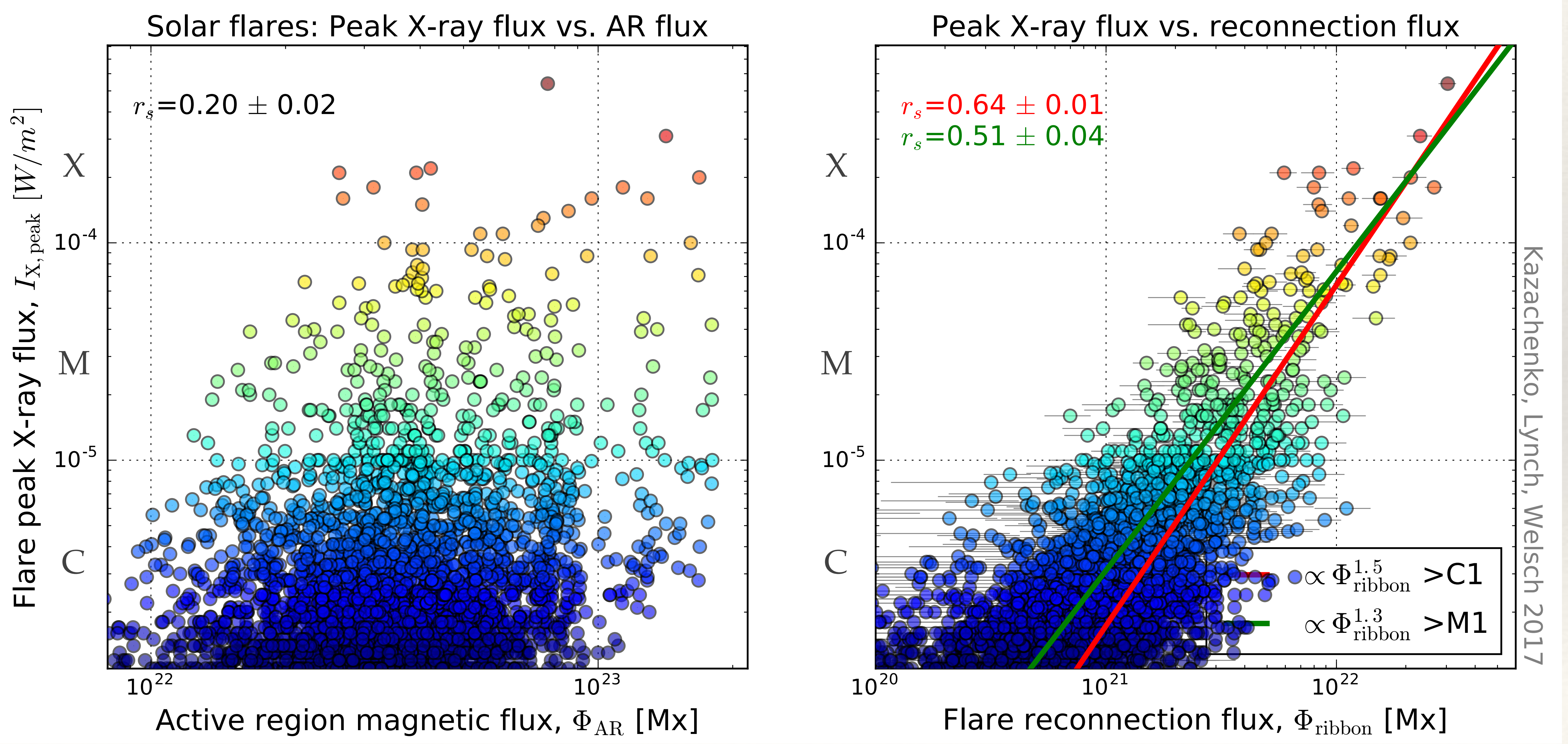

Results: Peak X-ray flux vs active region and ribbon areas

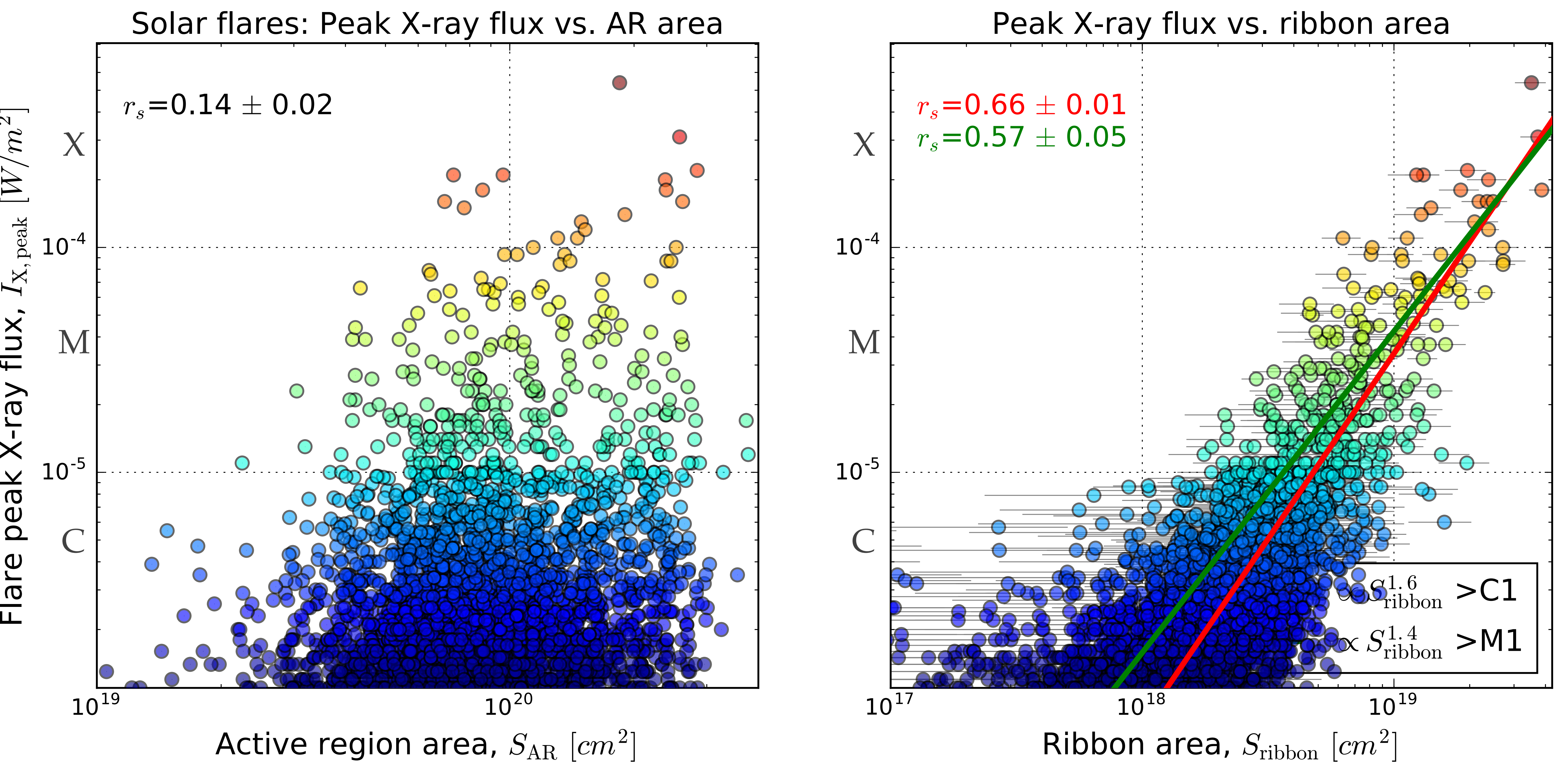

Results: mean magnetic field in ribbons and in active regions

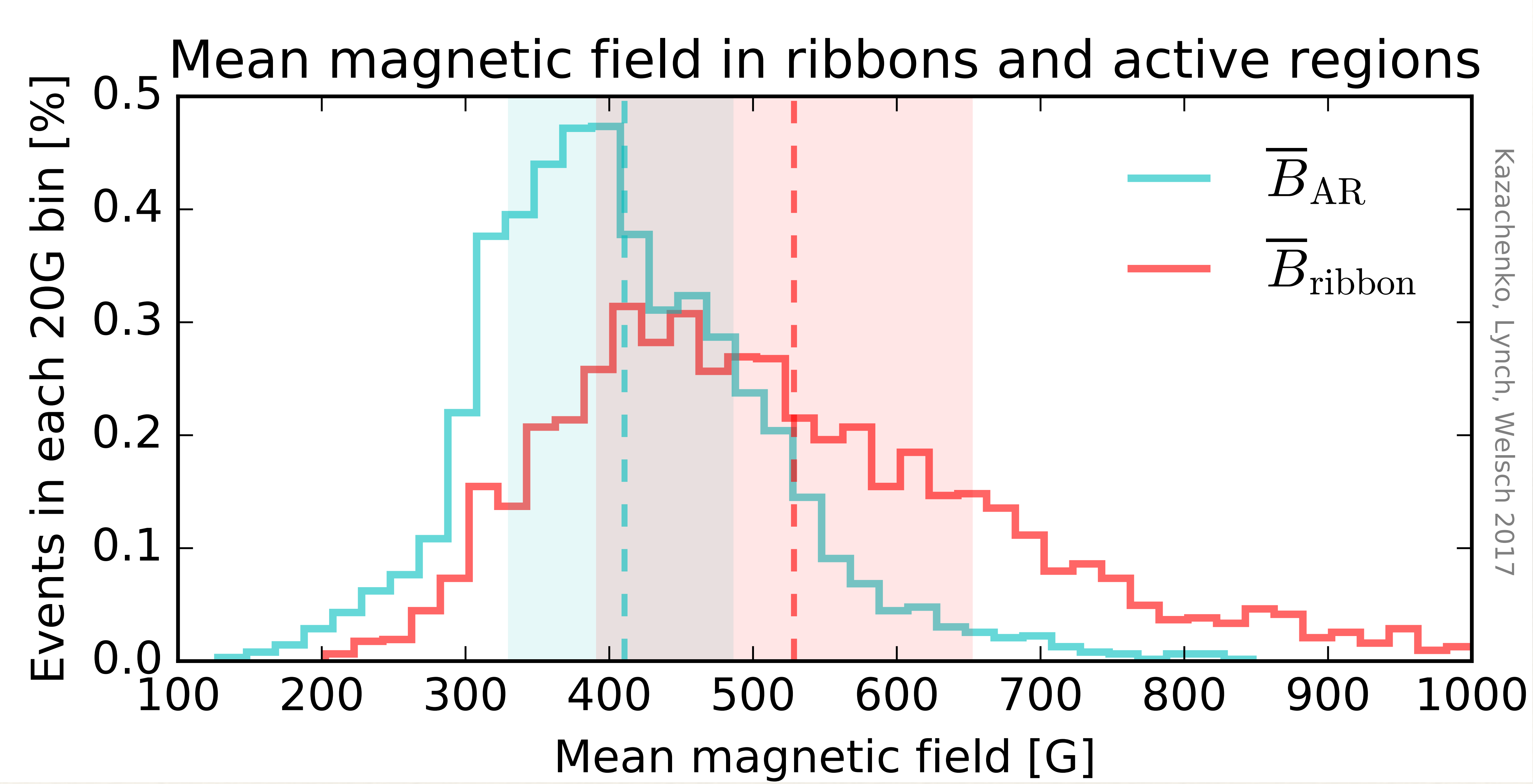

Results: Fraction of flux reconnected

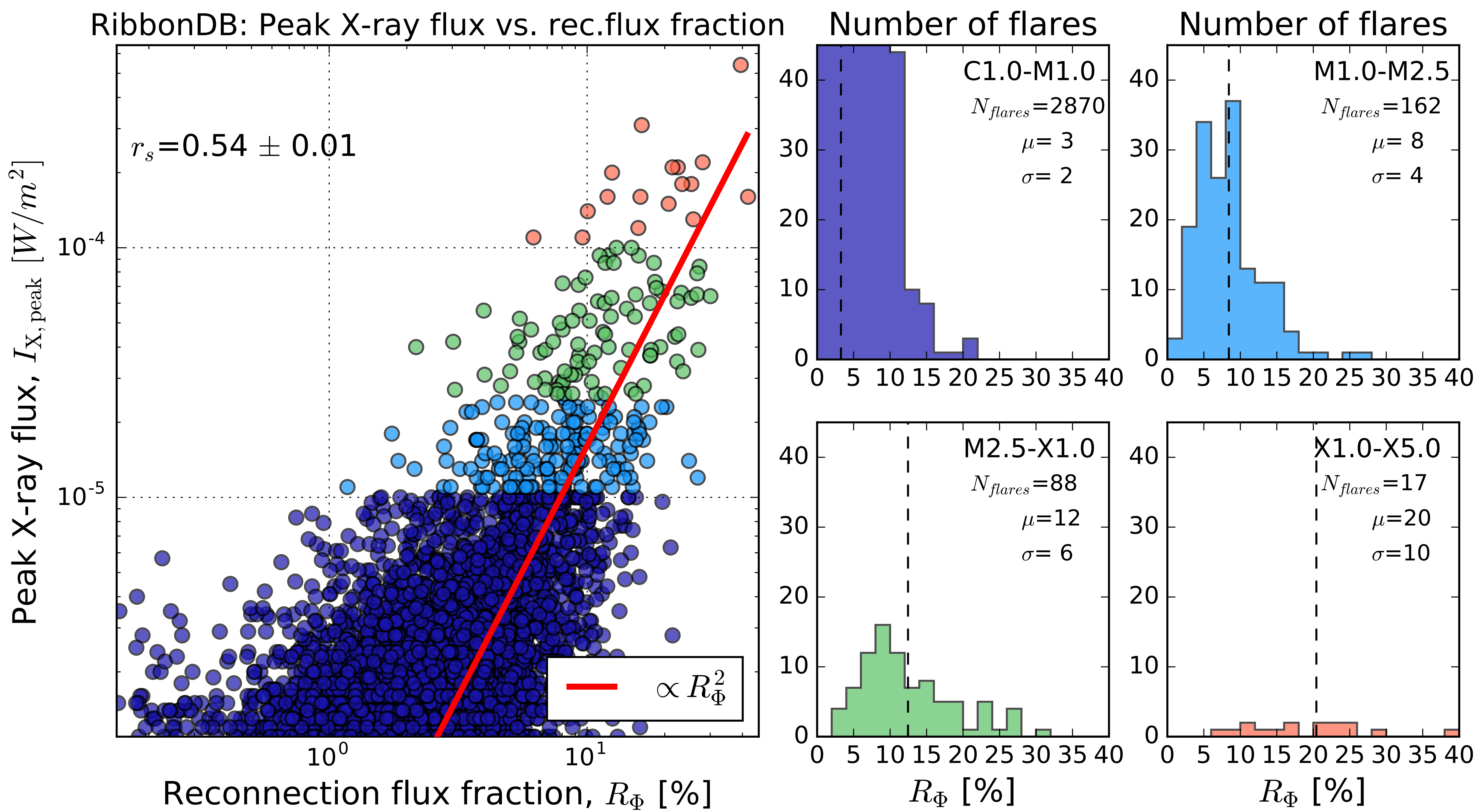

Summary table: peak X-ray flux vs active region and ribbon properties

ACTIVE REGIONS			FLARE RIBBONS				
	Typical range	Correlation		Typical range	Correlation	$I_{\mathrm{X,peak}}$	Fig.
$\mathbb{X}_{\mathrm{AR}}$	$[P_{20}, P_{80}]$	$r_s(\mathbb{X}_{\mathrm{AR}}, I_{\mathrm{X,peak}})$	$\mathbb{X}_{\mathrm{ribbon}}$	$[P_{20}, P_{80}]$	$r_s(\mathbb{X}_{\mathrm{ribbon}}, I_{\mathrm{X,peak}})$	$\propto$	
Φ_{AR}	$[23, 55]$ 10^{21} Mx	0.2 ± 0.02	Φ_{ribbon}	$[4.1, 1.8]$ 10^{21} Mx	0.64 ± 0.01	$\Phi_{\mathrm{ribbon}}^{1.5}$	Fig. 8
S_{AR}	$[57, 134]$ 10^{18} cm^2	0.14 ± 0.02	S_{ribbon}	$[0.9, 3.1]$ 10^{18} cm^2	0.66 ± 0.01	$S_{\mathrm{ribbon}}^{1.6}$	Fig. 9
B_{AR}	$[330, 474]$ G	0.18 ± 0.02	B_{ribbon}	$[404, 686]$ G	0.22 ± 0.02	–	Fig. 10
R_{Φ}	$[1.2, 5.1]$ %	0.54 ± 0.01	R_S	$[1.0, 3.8]$ %	0.54 ± 0.01	R_{Φ}^2	Fig. 11

Understanding observed scaling: $I_{X,Peak} \sim \Phi_{ribbon}^{1.5}$

From Warren & Antiochos (2004):

$$I_{\mathrm{X,peak}} \sim \frac{E_{flare}^{1.75}}{V^{0.75}L^{0.25}} \sim \frac{E_{flare}^{1.75}}{A_{\mathrm{ribbon}}^{\frac{5}{4}}}$$

since $V \sim L^3 \sim A_{\mathrm{ribbon}}^{3/2}$

On the other hand flare energy

$$E_{flare} \sim \frac{\int B_{rec}^2 dV}{8\pi} \sim \frac{\Phi_{\mathrm{ribbon}}^2}{8\pi L} \sim \frac{\Phi_{\mathrm{ribbon}}^2}{8\pi A_{\mathrm{ribbon}}^{1/2}}.$$

Hence peak X-ray flux

$$I_{\mathrm{X,peak}} \propto \frac{\Phi_{\mathrm{ribbon}}^{3.5}}{\Phi_{\mathrm{ribbon}}^{2\frac{1}{8}}} = \Phi_{\mathrm{ribbon}}^{1.3}$$

k=1.3

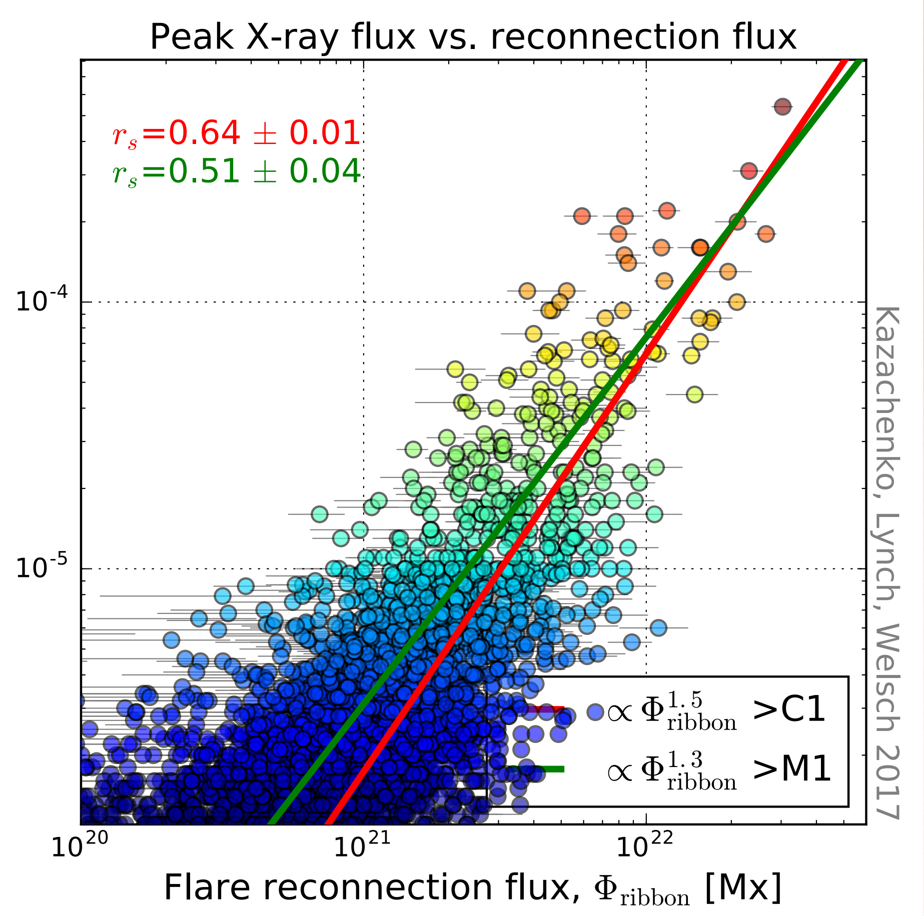

Kazachenko, Lynch, Welsch 2017

<u>From observations:</u>

k=1.5 for flares >C1.0

k=1.3 for flares >M1.0

Peaks X-ray Flux, Reconnection Flux, and Flare Magnetic Energy: Occurrence frequencies

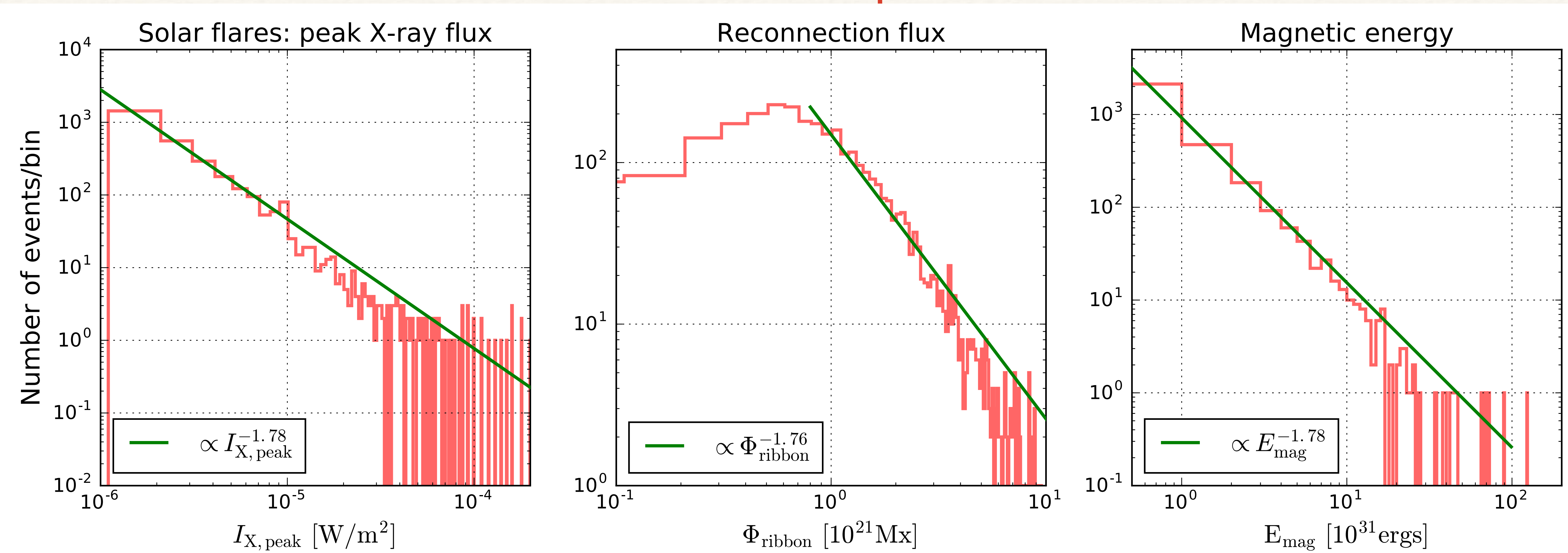

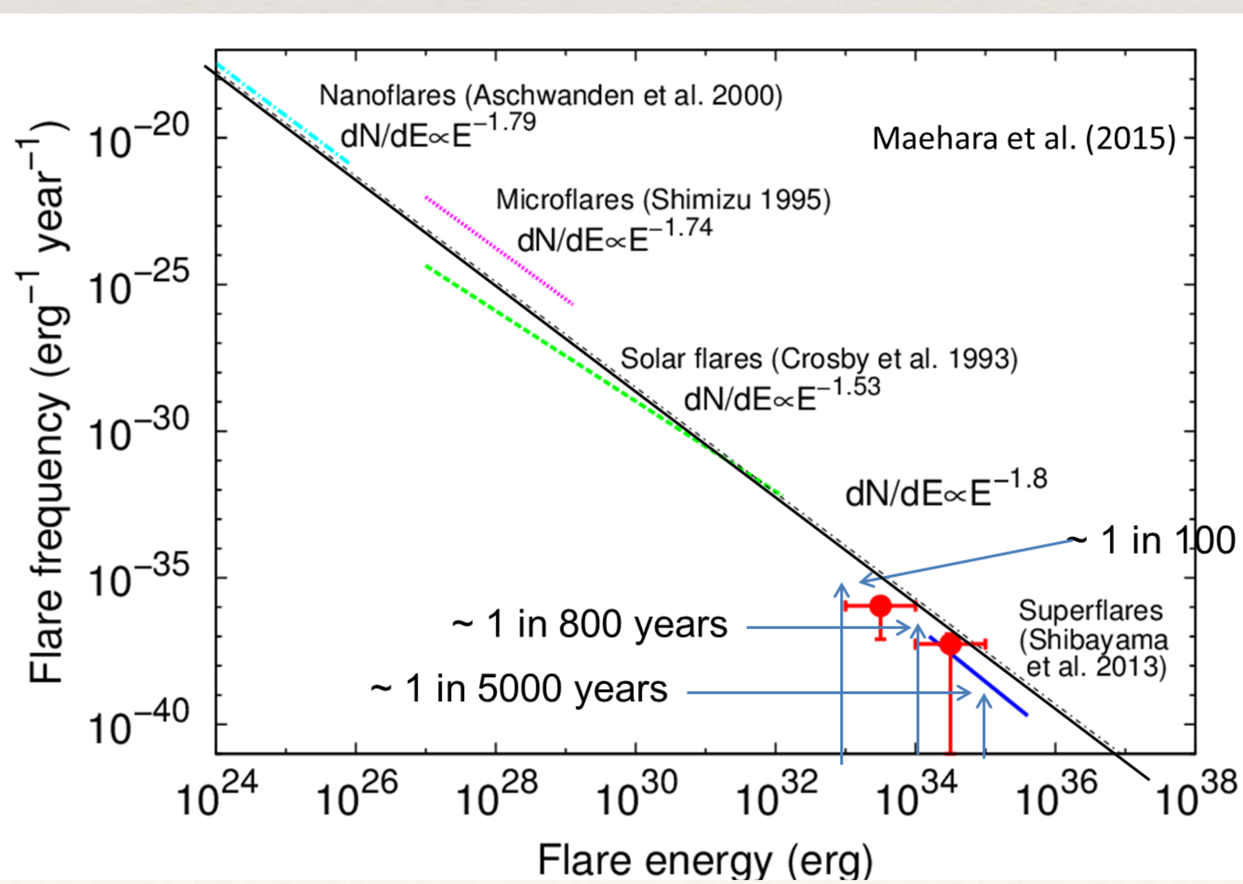

<u>Earlier solar flare observations:</u>

alpha=-1.5 - -1.8

<u>Stellar flares:</u>

apha= -1.8

<u>This work</u>

apha= -1.8

Summary

Database

We assembled a dataset of flare-ribbons reconnection fluxes for all flares, observed by SDO, C1.0 and larger, ~3000 events total.

Results

- Strong correlation between GOES flare class and reconnection flux ($I_{X,Peak} \sim \Phi_{ribbon}^{1.3\text{-}1.5}$) — "more reconnection flux results in larger flares"
- Strong correlation between GOES flare class and reconnection-flux fraction — "larger fraction of the magnetic flux that participates leads to larger flares"
- Above scaling law between peak X-ray flux and reconnection flux could constrain reconnection properties on other stars

Science Questions To Address With The Database

Almost all ribbons exhibit two-stage evolution:

- fast expansion along the PIL (“zipper-effect”)
- slow separation perpendicular to PIL

What is the mechanism of such division?

What is the relationship between flare ribbons and

- areas of strong vertical photospheric electric currents?
- areas of strong- and weak- shear?

- What is relationship between ribbons and CME/ICME properties?

Case study: 3D MHD Simulation of Eruptive Flare

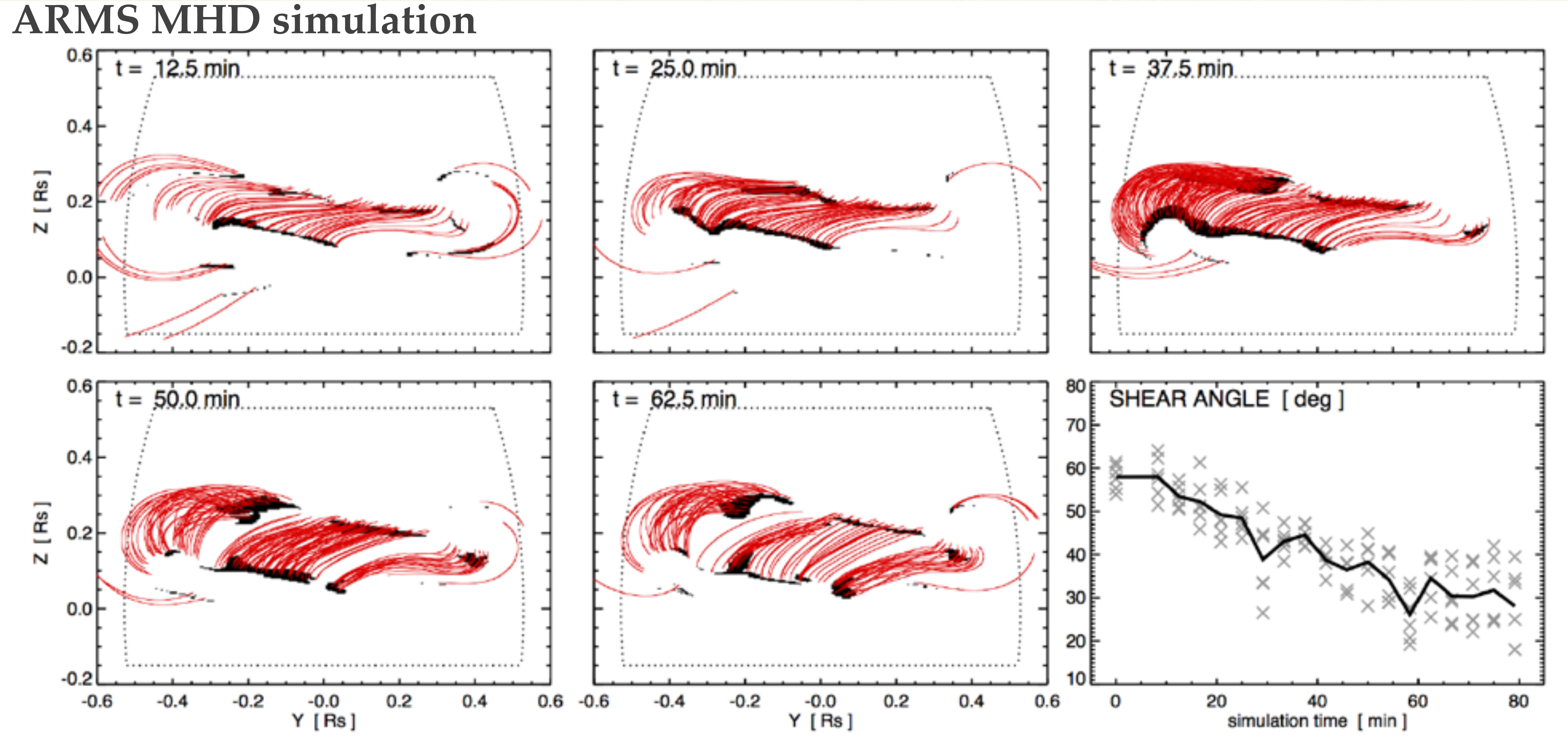

3D MHD Adaptively Refined MHD Solver (ARMS) simulation of a magnetic breakout eruption with a slow CME (Devore 1991, Lynch et al. 2008, 2009, 2014); 5 panels: evolution of post-eruption arcade (**Red**) and flare ribbons (post-eruption arcade footpoints, **Black**). **Bottom right:** evolution of post-eruption arcade shear relative to PIL; Note strong-to-weak shear transition.

In agreement with Su et al. 2007, Aulanier et al. 2012

Results: observations vs. simulations: flare-ribbons vs. vertical-currents

X2.2 flare observations

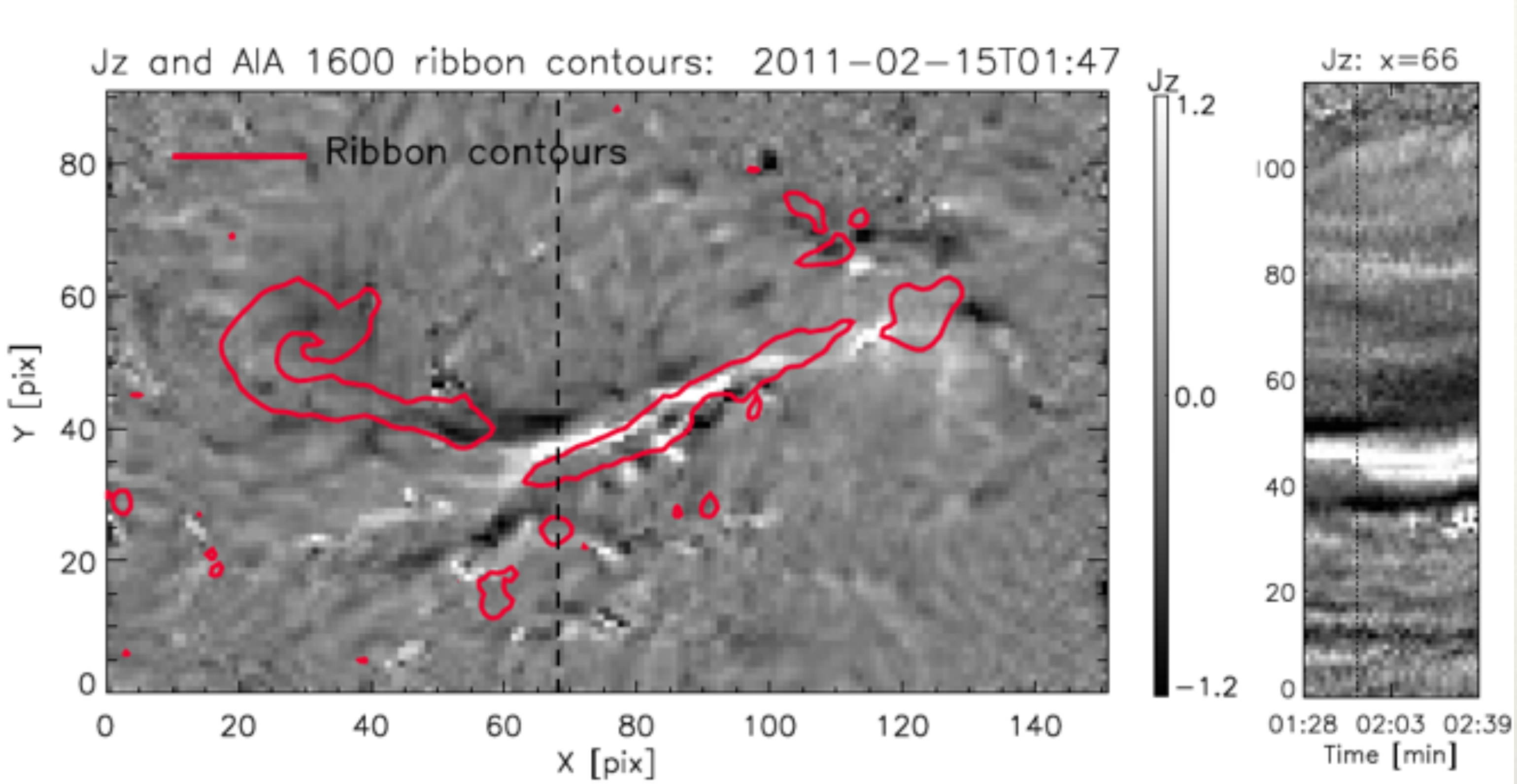

ARMS MHD simulations

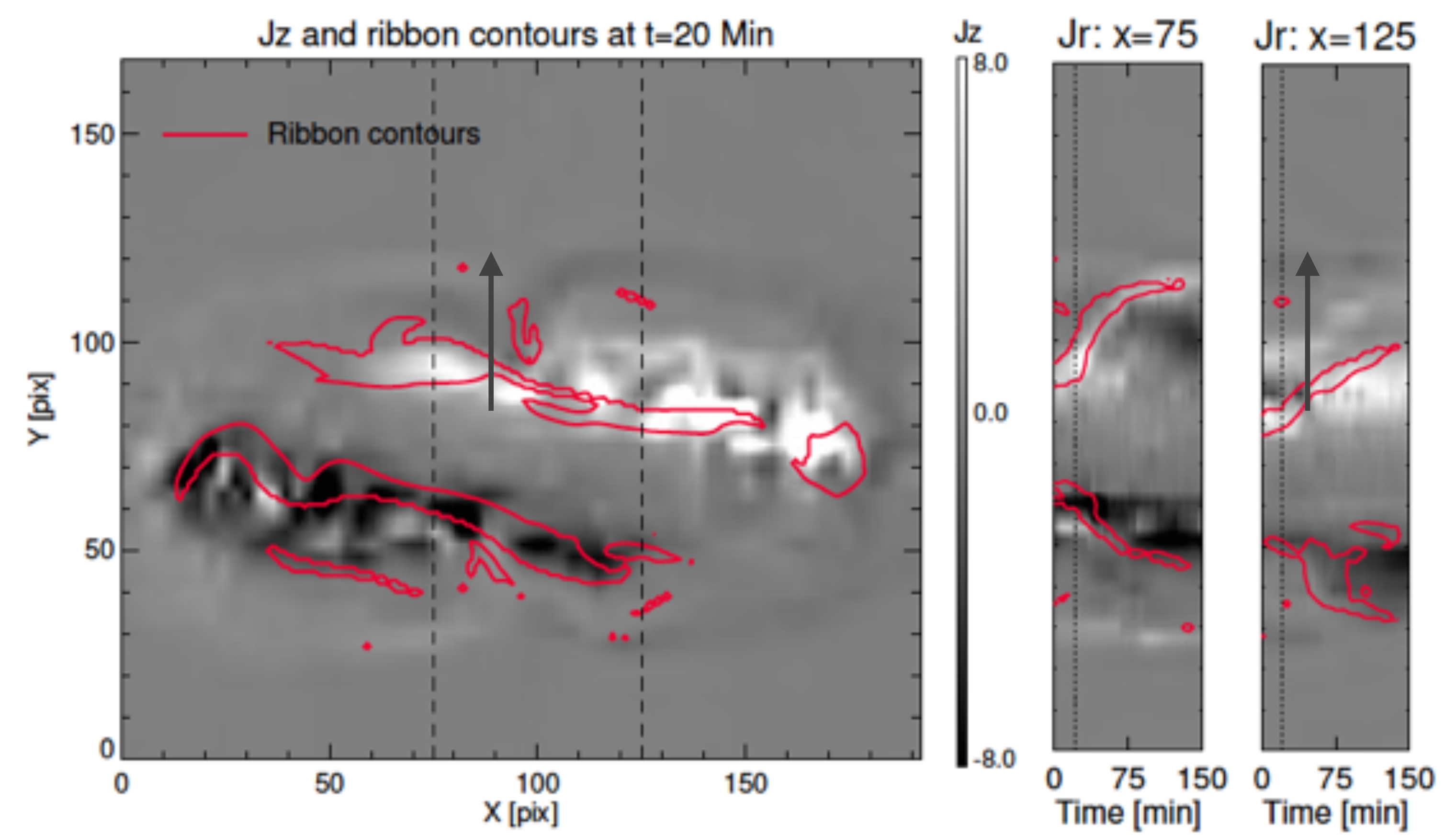

Left:
Vertical electric current Jz (Black) and flare ribbons contours (**Red**)

Right:
Temporal evolution of Jz and flare ribbons across vertical slits marked with dashed lines on the left from.

Results: observations vs. simulations: reconnection flux and CME speed/acceleration

X2.2 flare observations

ARMS MHD simulations

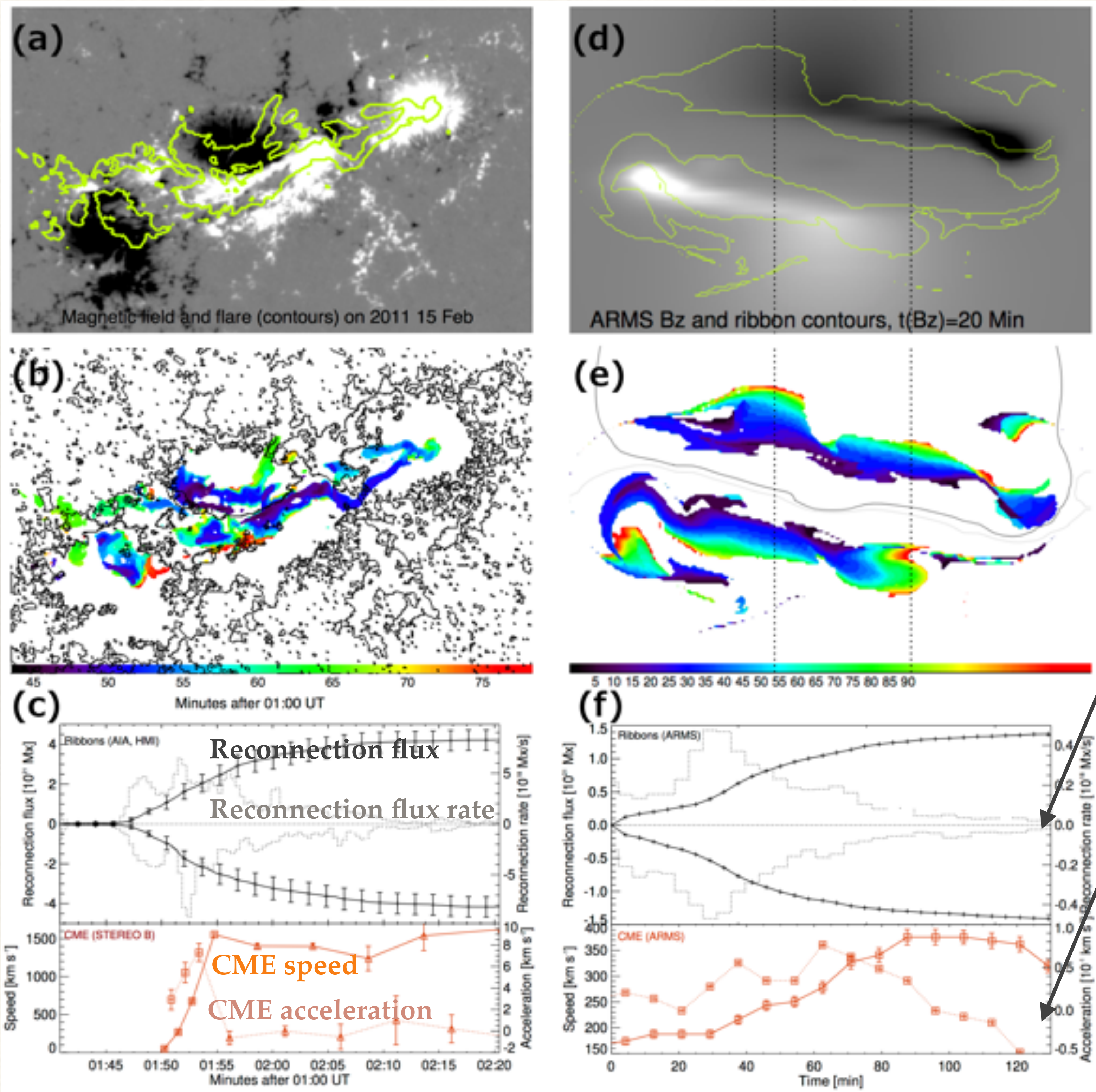

Green: Contours of the maximum flare ribbon area at the end of the ribbon image sequence

Black/white: Bz-magnetogram.

Color: Temporal evolution of cumulative ribbon maps

Black: time profiles of the total reconnection flux (solid) and the reconnection rate (dotted) in positive and negative polarities

Red: velocity (solid) and acceleration (dotted) profiles of the CME front from

- *observations (*STEREO-B observations (90 degrees apart from SDO, EUVI (squares) and COR1 (triangles)), *and*
- synthetic white light images from ARMS simulations.

Summary

Case study
We did a detailed study of flare-ribbon properties (geometry, reconnected-flux, high-cadence vertical-current evolution) of X2.2 flare in AR 11158 and compared these with properties of an ARMS MHD simulation.

Results: In both simulations and observations we find:

- Strong-to-weak shear evolutions
- Two-stage ribbon evolution
- Similar reconnection-flux temporal profiles
- Vertical-current enhancements near the flare ribbons

Thank you!